

Cite this: *Dalton Trans.*, 2017, **46**, 8350Received 8th April 2017,
Accepted 5th June 2017

DOI: 10.1039/c7dt01262d

rsc.li/dalton

A two-dimensional porous framework: solvent-induced structural transformation and selective adsorption towards malachite green†

Huanzhi Li,^a Xueting Fang,^a Sha Ma,^a Yanfei Niu,^b Xiaoli Zhao,^{ib} Jiaqiang Xu^{*a} and Zhiming Duan^{ib} ^{*a}

A two-dimensional porous framework SHU-1 could undergo solvent-induced structural transformations to SHU-1a in methanol and SHU-1b in water. SHU-1, SHU-1a and SHU-1b showed selective adsorption towards malachite green.

Metal–organic frameworks (MOFs), as an emerging class of porous materials, have been considered to be an intriguing platform to achieve a great variety of functionalities due to their distinctive advantages exhibited by pre-designed diverse, flexible and tunable porous structures.¹ Recently, more and more two-dimensional (2D) MOFs have received great attention for their structure diversity and flexibility.² 2D MOFs are usually maintained by weak interactions including hydrogen-bonding, π - π -stacking and van der Waals interactions, therefore, the structural integrity is easily broken, resulting in the total loss of crystallinity and porosity. Through interdigitation or interpenetration, the pore structure of 2D MOFs could be strengthened by π - π -stacking or C-H \cdots π interactions.³ Furthermore, the ligand rigidity could be imparted into the framework, and contribute to the retention of the pore structure after template or solvent removal.⁴ A large variety of rigid 2D MOFs have been reported, and only some of them showed single-crystal to single-crystal (SC-SC) transformation behavior.⁵ Among these SC-SC 2D MOFs, the observation of drastic changes in the layered structure is seldom recorded because of the difficulty in preserving the crystallinity.⁶

In this work, we present a new 2D framework **SHU-1** constructed *via* a combination of a bent dicarboxylate ligand 9,9'-spirobi[9*H*-fluorene]-2,2'-dicarboxylic acid (**H₂L**) and a novel

square-planar Ca₄O cluster, exhibiting a hollow layered structure. **SHU-1** could undergo solvent-induced structural transformations to **SHU-1a** in methanol and **SHU-1b** in water. Among these transformations, **SHU-1** transformed into **SHU-1a** *via* a single crystal to single crystal (SC-SC) fashion, and the transformations between **SHU-1a** and **SHU-1b** were reversible. **SHU-1**, **SHU-1a** and **SHU-1b** showed selective adsorption towards malachite green. To the best of our knowledge, **SHU-1** may be a rare example of rigid 2D MOFs showing drastic structural changes together with the preservation of crystallinity. It is noteworthy that the employment of light-weight and earth-abundant metal ions such as Ca²⁺ will facilitate the production of low-density/low-cost MOFs for the practical application. It is also well documented that Ca²⁺ with plenty of coordination modes is beneficial for the formation of different types of Ca²⁺-based MOFs.⁷ Besides, bent carboxylate ligands are widely used to implement the strategy of ligand symmetry modulation.⁸ As an ideal parent candidate for a bent ligand, there are limited reports on distinctive MOF structures containing a spiro-ligand,^{4b,9} let alone a systematic study of the influence of structural adjustment.

H₂L was selected and conveniently synthesized in two steps (Scheme S1, ESI†). The Friedel–Crafts acylation of 9,9'-spirobi[9*H*-fluorene], followed by sodium hypobromite oxidation and acidification could give rise to **H₂L-EtOH-H₂O**. The chemical structure of **H₂L** was unambiguously confirmed by NMR and MS (Fig. S1–S4, ESI†).

Colorless square plate-like crystals (Fig. S5a, ESI†) of **SHU-1** were solvothermally synthesized by the reaction of Ca(NO₃)₂·4H₂O and **H₂L** in DMF/MeOH solution. **SHU-1** could be formulated as [(CH₃)₂NH₂]₂[(Ca₄O)L₄(H₂O)₄]₆DMF based on single crystal X-ray structure analysis in combination with thermogravimetric analysis (TGA) and elemental analysis.

Single crystal X-ray diffraction analysis revealed that **SHU-1** crystallizes in the tetragonal space group *I4/m* (Table S1, ESI†). The framework of **SHU-1** consists of 2D layers, in which square-planar Ca₄O clusters are linked by ligands. The Ca and O atoms of the Ca₄O cluster are located at *8h* and *2b* Wyckoff positions, and the spiro-carbon (C8) of the ligand occupies the

^aDepartment of Chemistry, College of Sciences, Shanghai University, Shanghai 200444, P. R. China. E-mail: duanzm@shu.edu.cn, xujiaqiang@shu.edu.cn; Tel: +86-21-66138002

^bShanghai Key Laboratory of Green Chemistry and Chemical Processes, Department of Chemistry, East China Normal University, Shanghai 200062, P. R. China

† Electronic supplementary information (ESI) available: Experimental details, synthesis and characterization, crystallographic data, TGA, PXRD, dye adsorption, and additional figures and details. CCDC 1424463, 1470061 and 1552733. For ESI and crystallographic data in CIF or other electronic format see DOI: 10.1039/c7dt01262d

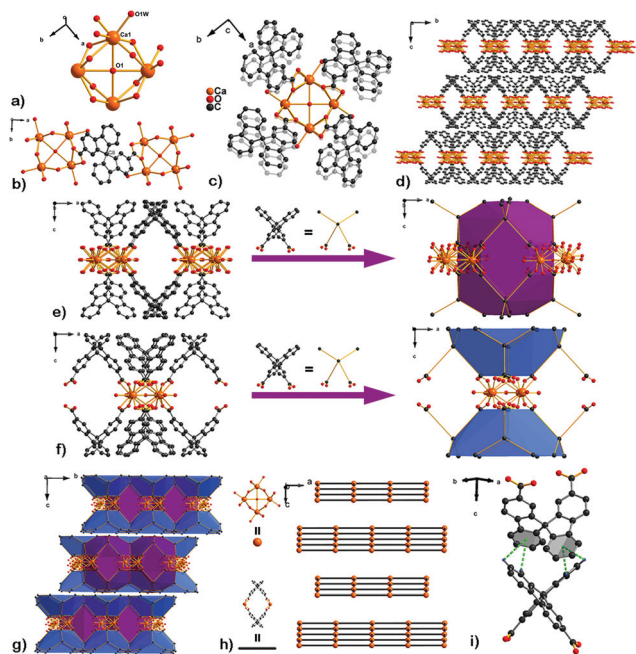


Fig. 1 (a) The coordination environment of Ca^{2+} . (b) The connection of the ligand. (c) Square planar Ca_4O cluster. (d) The 2D hollow layered structure of **SHU-1** viewed along the a axis. (e) The representation of a cage-like void. (f) The representation of an hourglass-shaped void. (g) The arrangement of two kinds of voids. (h) The topology and packing mode of **SHU-1**. (i) $\text{C-H}\cdots\pi$ interactions of **SHU-1** (green dashed lines, distance: 3.52–3.73 Å, measured between H and adjacent phenyl ring centroids).

$2b$ Wyckoff position. Ca^{2+} ion takes a distorted octa-coordinated geometry with six O atoms from four ligands, one O atom from terminal H_2O and one O atom from cluster (Fig. 1a). The ligand is connected to two Ca^{2+} ions from two Ca_4O clusters *via* O atoms from carboxylates (Fig. 1b). The unique tetranuclear Ca_4O cluster is composed of one central O atom and four Ca^{2+} ions giving a Ca-O distance of 2.697(2) Å, a $\text{Ca}\cdots\text{Ca}$ distance of 3.814(3) Å, and the Ca-O-Ca angles of 90° and 180° (Fig. 1c). Each Ca_4O cluster connects to its four neighbors *via* eight ligands to form a 2D hollow layer (Fig. 1d). In each layer, four Ca_4O clusters and eight ligands join together to form a cage structure (Fig. 1e), and these cages extend along both a and b axes by sharing rhombic windows with the dimension of $4.3 \text{ \AA} \times 10.2 \text{ \AA}$. Besides, there exist hourglass-shaped voids defined by one Ca_4O cluster and eight ligands (Fig. 1f). Two types of voids are arranged alternately (Fig. 1g). The layers could be considered as (4,4) grids, and they take a staggered stacking mode (AB stacking) along the c axis to afford the whole framework (Fig. 1h). The $\text{Ar-H}\cdots\text{Ar}$ distance of 3.52–3.73 Å measured between the adjacent layers indicates weak $\text{C-H}\cdots\pi$ interactions (Fig. 1i). The void volume calculated by PLATON is 41.1% of the unit cell volume upon removal of guest molecules, which is comparable to 3D frameworks constructed from similar tetranuclear transition metal clusters.¹⁰

Crystals of **SHU-1** undergo a single crystal to single crystal (SC-SC) transformation when soaked in dry methanol for 48 h

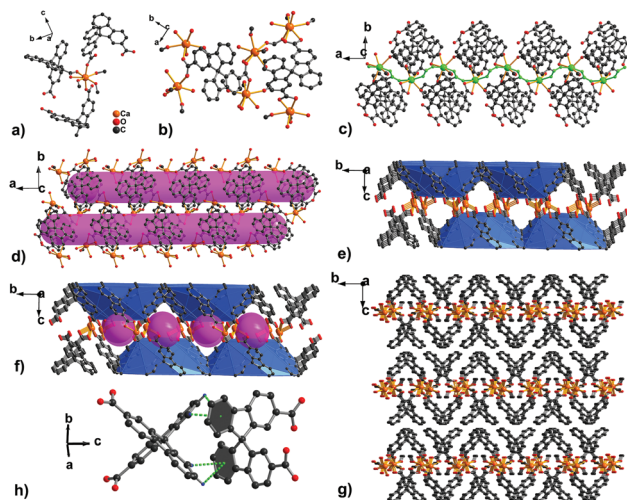


Fig. 2 (a) The coordination environment of Ca^{2+} . (b) η_2 and *syn-anti* bridging modes of the ligand. (c) The zig-zag chain of Ca^{2+} indicated by the green color. (d) 1D tubular structure in the layer of **SHU-1a**. (e) The bowl-shaped voids in the layer of **SHU-1a**. (f) The arrangement of tubular pores and bowl-shaped voids. (g) The 2D hollow layered structure of **SHU-1a** viewed along the a axis. (h) $\text{C-H}\cdots\pi$ interactions of **SHU-1a** (green dashed lines, distance: 2.74–3.55 Å, measured between H and adjacent phenyl ring centroids).

(Fig. S15, ESI†). The resulting colorless plate-like crystals of **SHU-1a** were obtained (Fig. S5b, ESI†), and the structure of **SHU-1a** could be solved successfully. **SHU-1a** crystallizes in the orthorhombic space group $Pccn$ (Table S1, ESI†), and the 2D structure is extended along the ab plane in the framework of **SHU-1a**. The Ca atoms and spiro-carbon atoms are separately located at $8e$ and $4c$ Wyckoff positions. The Ca^{2+} ion is hepta-coordinated by four O atoms from three ligands and three O atoms from MeOH with a distorted pentagonal bipyramid geometry (Fig. 2a). The ligands act as bidentate bridges in two manners. One is that two carboxylate groups of the ligand bridge neighboring Ca^{2+} ions in a η_2 mode with a $\text{Ca}\cdots\text{Ca}$ distance of 10.864(2) Å, the other is that two carboxylate groups connect neighboring Ca^{2+} ions in a *syn-anti* configuration with a $\text{Ca}\cdots\text{Ca}$ distance of 5.534(2) Å (Fig. 2b), forming a 1D zig-zag chain along a axis (Fig. 2c). These ligands are evenly distributed around the zig-zag chains, and link them into a 2D layer with 1D tubular pores (Fig. 2d). The dimensions of the tubular pores are calculated to be *ca.* $8.6 \text{ \AA} \times 6.1 \text{ \AA}$ along the a axis. In each layer, the bowl-shaped voids defined by four ligands are located above and below the tubular pores in a staggered arrangement (Fig. 2e and f). These layers stack together in overlay mode along the c axis to form the overall framework (Fig. 2g). The $\text{Ar-H}\cdots\text{Ar}$ distance of 2.74–3.55 Å measured between the adjacent layers is shorter than that found in **SHU-1**, indicating slightly strong $\text{C-H}\cdots\pi$ interactions (Fig. 2h). The solvent accessible void is 33.3% of the crystal volume after removal of the guest and coordinated solvent molecules, calculated by PLATON.

Both **SHU-1** and **SHU-1a** were unstable in water, and they transformed into a new crystalline phase **SHU-1b** (Fig. S5c,

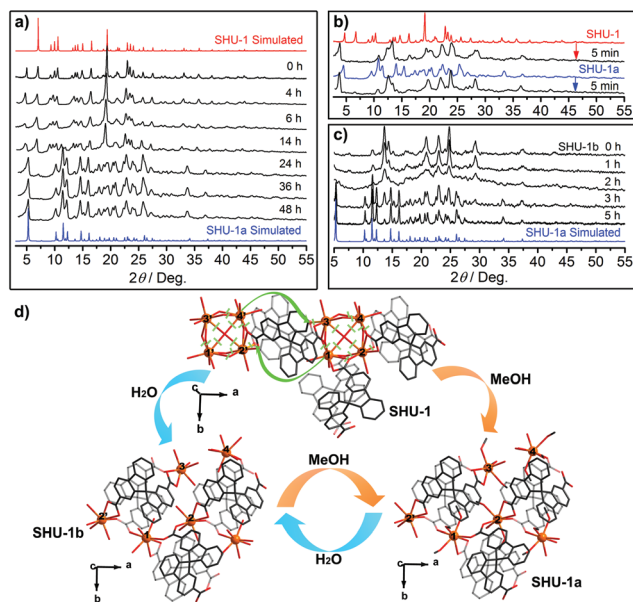


Fig. 3 (a) The PXRD patterns monitored during the SC–SC transformation from SHU-1 to SHU-1a. (b) The PXRD patterns monitored during the structural transformations of SHU-1 to SHU-1b and SHU-1a to SHU-1b. (c) The PXRD patterns monitored during the structural transformation from SHU-1b to SHU-1a. (d) Proposed mechanism for structural interconversions among SHU-1, SHU-1a and SHU-1b.

ESI[†]). Unfortunately, the resulting sample was unsuitable for single crystal X-ray diffraction. To probe the structure of SHU-1b, the dried sample of SHU-1b was left undisturbed in methanol. Interestingly, SHU-1b could be re-transformed into SHU-1a in several hours. Combining with TGA and elemental analysis results, we would like to speculate that the 2D layered structure was retained in SHU-1b, and the exchange of the coordinated solvent may be involved in structural transformation without affecting the integrity of the network.

To gain more detailed insight into the structural interconversion among SHU-1, SHU-1a and SHU-1b, powder X-ray diffraction (PXRD) was monitored during the process of transformation. As shown in Fig. 3a, SHU-1 showed diffraction peaks around the 2θ angles of 7.05, 9.97, 13.66, 14.99, 16.58 and 19.37 degrees. When SHU-1 was soaked in methanol, there were almost no changes in the position of the diffraction peaks, while the peak broadening had been observed in 6 h. The peaks around the 2θ angles of 10.24, 11.52, 12.27, 14.72 and 16.14 degrees corresponding to SHU-1a appeared after 14 h. The peaks corresponding to SHU-1 disappeared after 24 h, and the PXRD pattern was coincident with that of SHU-1a simulated from single crystal diffraction data, indicating that the structure of SHU-1 was fully converted into that of SHU-1a in methanol. When SHU-1 and SHU-1a were soaked in water, both of them could be converted into SHU-1b in several minutes as shown in Fig. 3b. When the dried sample of SHU-1b was soaked in methanol, a slightly blurred diffraction pattern was observed after 2 h, and clear peaks corresponding to SHU-1a appeared after 5 h (Fig. 3c). A possible mechanism

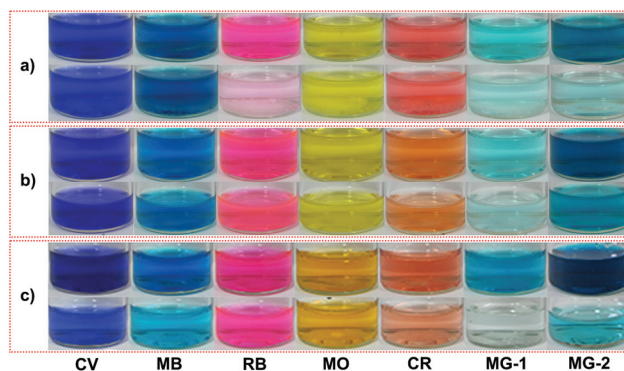


Fig. 4 Color comparisons before (upper panel) and after (lower panel) dye adsorption on (a) SHU-1 in acetone, (b) SHU-1a in methanol, (c) SHU-1b in water. The initial concentration: CV, MB, RB, MO, CR, MG-1, $5.00 \times 10^{-5} \text{ mol L}^{-1}$; MG-2, $4.00 \times 10^{-4} \text{ mol L}^{-1}$ for SHU-1 and SHU-1a, $8.00 \times 10^{-4} \text{ mol L}^{-1}$ for SHU-1b.

for these structural interconversions has been proposed as shown in Fig. 3d. The transformation starts with a cleavage of the Ca_4O cluster of SHU-1 through Ca–O bonds, induced by solvents. As indicated in Fig. 3d, Ca^{2+} ions in one Ca_4O cluster move apart from each other, and get close to the Ca^{2+} ions in the neighboring Ca_4O cluster to form new Ca–O bonds in η_2 or *syn-anti* mode. At the same time, the above step triggers the rotation of the ligands to receive the approaching Ca^{2+} ions. Concerning the transformation between SHU-1a and SHU-1b, the coordinated solvents may be exchanged in methanol or water, and the 2D layered framework could be maintained.

In order to testify the void accessibility, the dye adsorption experiments were separately carried out in acetone for SHU-1, methanol for SHU-1a and water for SHU-1b. The PXRD patterns of SHU-1, SHU-1a and SHU-1b remained unchanged after dye adsorption (Fig. S9, ESI[†]). A series of dyes including cationic crystal violet (CV), methylene blue (MB), rhodamine-B (RB) and malachite green (MG), and anionic methyl orange (MO) and Congo red (CR) were chosen as the typical models considering their charges and geometry sizes. UV-vis spectroscopic results exhibited that SHU-1, SHU-1a and SHU-1b showed selective adsorption towards MG (Fig. 4 and S11, ESI[†]). Apparently, the cyan solution of MG faded away more rapidly than any other dye. Typically, 30.0 mg of SHU-1, SHU-1a or SHU-1b was soaked and shaken in 4 mL of solution ($5.00 \times 10^{-5} \text{ mol L}^{-1}$) for each of the above dyes at room temperature. SHU-1 showed the adsorption capacity of 6.67 mol g^{-1} (2.43 mg g^{-1}) towards MG in acetone, and the values were 4.33 mol g^{-1} (1.58 mg g^{-1}) for SHU-1a in methanol, and 6.33 mol g^{-1} (2.30 mg g^{-1}) for SHU-1b in water, respectively. The maximal adsorption capacities of 51.5 mol g^{-1} (18.8 mg g^{-1}) for SHU-1, 40.6 mol g^{-1} (14.8 mg g^{-1}) for SHU-1a, and 94.4 mol g^{-1} (34.5 mg g^{-1}) for SHU-1b could be achieved, when the initial concentration of MG was increased to $4.00 \times 10^{-4} \text{ mol L}^{-1}$ for SHU-1 and SHU-1a, and $8.00 \times 10^{-4} \text{ mol L}^{-1}$ for SHU-1b (Table S2, ESI[†]). For the practical application of treating dye-containing wastewater, the adsorption capacity of

SHU-1b is higher than those of commercial activated carbon and natural zeolite, and very close to that of MIL-53, but lower than those of chitosan bead and MIL-100(Fe) (Table S3, ESI†).¹¹

The selective adsorption of MG on **SHU-1**, **SHU-1a** and **SHU-1b** may be attributed to the synergistic effect of size exclusion and acid–base interaction. The hollow layered structure may accommodate the MG molecule, and MG could partially insert its phenyl group into the windows of the layer. Furthermore, this kind of insertion may be favored by the π – π interaction between the phenyl group of MG and the aromatic backbone of **SHU-1**, **SHU-1a** and **SHU-1b**. The Lewis acid–base interaction may also play an important role in the selective adsorption. The Lewis acid site of the Ca^{2+} atom could interact with the Lewis base group $-\text{N}(\text{CH}_3)_2$ of MG after the replacement of coordinated solvents. More open metal sites could be obtained in water for **SHU-1b**, therefore **SHU-1b** showed higher adsorption capacity than those of **SHU-1** and **SHU-1a**. The geometry size and ionic strength of MG may match well with the specific void structure of **SHU-1**, **SHU-1a** and **SHU-1b**, and contribute to the selective adsorption. Besides, a preliminary study revealed that an ion-exchange mechanism may be involved in the process of adsorption for **SHU-1** (Fig. S10 and S13, ESI†).

In conclusion, we have disclosed solvent-induced structural transformations that take place among rigid 2D MOFs. Drastic changes in the layered structure have been observed during the SC–SC transformation process from **SHU-1** to **SHU-1a**, meanwhile a reversible structural transformation has been discovered between **SHU-1a** and **SHU-1b**. Furthermore, **SHU-1**, **SHU-1a** and **SHU-1b** have shown the void accessibility by selective adsorption towards MG. More investigations on tuning the structure diversity of spirobifluorene-based MOFs *via* the adjustment of ligand rigidity and flexibility remain to be conducted.

This work was financially supported by the National Natural Science Foundation of China (21201118 & 61371021). Dr Min Shao, Dr Hongmei Deng, Dr Hui Zhang and Dr Bo Lu at the Instrumental Analysis and Research Center of Shanghai University are acknowledged for their assistance with measurements. We thank Prof. Zengqiang Gao from the Institute of High Energy Physics, Chinese Academy of Sciences for his kind help on synchrotron data reduction. We also thank the staff from beamlines 3W1A and 1W2B at the Beijing Synchrotron Radiation Facility (BSRF) for their assistance with data collection of **SHU-1a**.

Notes and references

- (a) W. Lu, Z. Wei, Z.-Y. Gu, T.-F. Liu, J. Park, J. Park, J. Tian, M. Zhang, Q. Zhang, T. Gentle III, M. Bosch and H.-C. Zhou, *Chem. Soc. Rev.*, 2014, **43**, 5561; (b) Y. He, B. Li, M. O’Keeffe and B. Chen, *Chem. Soc. Rev.*, 2014, **43**, 5618; (c) J.-P. Zhang, Y.-B. Zhang, J.-B. Lin and X.-M. Chen, *Chem. Rev.*, 2012, **112**, 1001.
- (a) W. J. Roth, P. Nachtigall, R. E. Morris and J. Čejka, *Chem. Rev.*, 2014, **114**, 4807; (b) X.-M. Liu, R.-B. Lin, J.-P. Zhang and X.-M. Chen, *Inorg. Chem.*, 2012, **51**, 5686.
- (a) R. Chen, J. Yao, Q. Gu, S. Smeets, C. Baerlocher, H. Gu, D. Zhu, W. Morris, O. M. Yaghi and H. Wang, *Chem. Commun.*, 2013, **49**, 9500; (b) I.-H. Park, H. Ju, T. S. Herng, Y. Kang, S. S. Lee, J. Ding and J. J. Vittal, *Cryst. Growth Des.*, 2016, **16**, 7278.
- (a) M. Zhang, G. Feng, Z. Song, Y.-P. Zhou, H.-Y. Chao, D. Yuan, T. T. Y. Tan, Z. Guo, Z. Hu, B. Z. Tang, B. Liu and D. Zhao, *J. Am. Chem. Soc.*, 2014, **136**, 7241; (b) L. An, H. Wang, F. Xu, X.-L. Wang, F. Wang and J. Li, *Inorg. Chem.*, 2016, **55**, 12923; (c) F. Ahmed, S. Roy, K. Naskar, C. Sinha, S. M. Alam, S. Kundu, J. J. Vittal and M. H. Mir, *Cryst. Growth Des.*, 2016, **16**, 5514.
- (a) Y. Wang, J.-M. Yi, M.-Y. Zhang, P. Xu and X.-J. Zhao, *Chem. Commun.*, 2016, **52**, 3099; (b) D. Liu, H.-F. Wang, B. F. Abrahams and J.-P. Lang, *Chem. Commun.*, 2014, **50**, 3173.
- J. Albalad, J. Aríñez-Soriano, J. Vidal-Gancedo, V. Lloveras, J. Juanhuix, I. Imaz, N. Aliaga-Alcaldebe and D. MasPOCH, *Chem. Commun.*, 2016, **52**, 13397.
- (a) K. Noh, N. Ko, H. J. Park, S. Y. Park and J. Kim, *CrystEngComm*, 2014, **16**, 8664; (b) D. Banerjee, Z. Zhang, A. M. Plonka, J. Li and J. B. Parise, *Cryst. Growth Des.*, 2012, **12**, 2162.
- (a) J. Pang, F. Jiang, M. Wu, D. Yuan, K. Zhou, J. Qian, K. Su and M. Hong, *Chem. Commun.*, 2014, **50**, 2834; (b) Y. Xie, H. Yang, Z. U. Wang, Y. Liu, H.-C. Zhou and J.-R. Li, *Chem. Commun.*, 2014, **50**, 563.
- (a) F. Moreau, N. Audebrand, C. Poriel, V. Moizan-Basle and J. Ouvry, *J. Mater. Chem.*, 2011, **21**, 18715; (b) P. K. Clews, R. E. Douthwaite, B. M. Kariuki, T. Moore and M. Taboada, *Cryst. Growth Des.*, 2006, **6**, 1991.
- (a) D. Chen, W. Shi and P. Cheng, *Chem. Commun.*, 2015, **51**, 370; (b) R. Hailili, L. Wang, J. Qv, R. Yao, X.-M. Zhang and H. Liu, *Inorg. Chem.*, 2015, **54**, 3713.
- S.-H. Huo and X.-P. Yan, *J. Mater. Chem.*, 2012, **22**, 7449.